ELSEVIER

Biophysical Chemistry 126 (2007) 36–42

Biophysical Chemistry

http://www.elsevier.com/locate/biophyschem

Characterization of intramolecular interactions of HIV-1 accessory protein Nef by differential scanning calorimetry

Teresa D. Groesch, Ernesto Freire *

Department of Biology, Johns Hopkins University, 3400 Charles Street, Baltimore, MD 21218, United States

Received 13 March 2006; received in revised form 10 May 2006; accepted 10 May 2006
Available online 30 May 2006

Abstract

The interactions between the N-terminal arm and the structural core of Nef, an HIV-1 accessory protein, have been studied by high sensitivity differential scanning calorimetry. Critical interactions have been identified by measuring the structural energetics of both truncation and point mutants of the protein. These studies demonstrate that the N-terminal arm of Nef strongly interacts with the core and that it contributes close to 4.3 kcal/mol to the stability of the entire protein. The interactions are not evenly distributed through the N-terminal arm. Two strongly interacting regions have been identified: the region between residues 1 and 40 that contributes 1.6 kcal/mol to the stability of Nef; and, the region between residues 50 and 61 that contributes 2.7 kcal/mol. Other regions (e.g. residues 41 to 49) appear to contribute little to the interaction. The identification of these, until now, elusive interactions provides a physical foundation for allosteric effects between N-terminal arm and protein core elicited by different binding partners.
© 2006 Elsevier B.V. All rights reserved.

Keywords: Differential scanning calorimetry; Nef; HIV; AIDS; Intraprotein interaction

1. Introduction

The HIV-1 accessory protein Nef has been shown to be important for the progression of HIV-1 infection to AIDS [1–3], but the exact role of Nef in the virus lifecycle is still not fully understood. Studies have implicated Nef in almost every step such as virus replication and infectivity, viral DNA integration, avoidance of immune detection, and modulation of cell signaling, but conflicting results due to the absence of good model systems have made it difficult to determine the exact mechanism of Nef during HIV-1 infection [4,5].

Nef is an adapter protein with no intrinsic enzymatic activity. In infected T-cells, Nef is myristoylated, and its association with the cellular membrane has been shown to be important for many of its proposed functions [6–8]. Nef is a 23 kDa protein composed of a compact core region, a flexible N-terminal arm (residues 1–69) and a large internal unstructured loop (residues 147–179). The structure of the core region of Nef has been solved by both X-ray crystallographic and NMR methods, but in both cases the N-terminal arm and the flexible loop from residues 147–179 were not present in the constructs (Fig. 1) [9–12].

The flexible regions of Nef are believed to be important to its role as an adapter protein since Nef has been shown to interact with a surprisingly large number of different proteins with a large variety of binding modes [13]. The presence of flexible regions facilitates structural rearrangements necessary for exposing different binding epitopes and for allosteric regulation of binding partners [13,14].

One example of allosteric regulation is the increase in binding affinity of Nef for the cytoplasmic tail of the CD4 receptor upon binding to the SH3 domain of Hck, a Src family kinase [15]. The Nef binding site to CD4 involves residues from both the N-terminal arm (W57, L58, and E59) as well as residues from the core of the protein (G95, G96, L97, R106, and L110) [15]. A naturally occurring mutation in Nef at the CD4 binding site, A56D, inhibits the down-regulation of CD4 and leads to a lengthening of the time between infection and development of full-blown AIDS, highlighting the importance of the interaction between Nef and CD4 [16–19]. Mutations at W57 and L58 (W57A and L58A) or the double mutant also

* Corresponding author. Tel.: +1 410 516 7743; fax: +1 410 516 6469.
E-mail address: ef@jhu.edu (E. Freire).

0301-4622/$ - see front matter © 2006 Elsevier B.V. All rights reserved.
doi:10.1016/j.bpc.2006.05.007

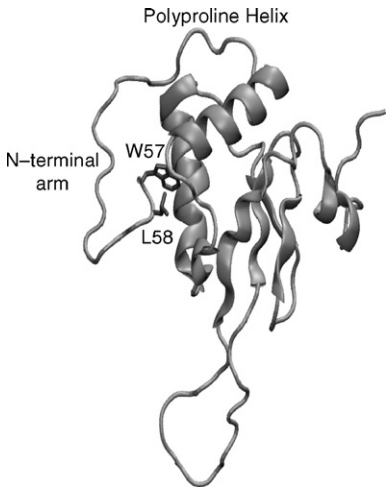

Fig. 1. Ribbon diagram of Nef. The NMR structure of Nef (pdb file 2NEF) beginning at residue 56 is shown [10,11]. The flexible N-terminal arm of Nef is labeled as well as the polyproline helix that marks the beginning of the structural core of the protein. Residues W57 and L58, which represent the relatively more rigid region of the N-terminus, are highlighted.

prevent the down-regulation of CD4 by Nef [20]. Another important binding region in Nef is the polyproline helix region (residues 69 to 79, shown in Fig. 1), immediately following the N-terminal arm in sequence, which binds SH3 domains of several Src family kinases [9,21].

Analysis of the backbone dynamics of Nef using NMR techniques indicates that the N-terminal arm is rather flexible up to around residue 69, which is the beginning of the polyproline helix [10,11]. While most of the N-terminal arm is highly flexible, there is a region of relative rigidity around the CD4 binding site (residues 53 to 60) and specifically residues W57 and L58. NMR experiments identify several NOE contacts in the structure that reveal a connection between residues W57 and L58 and a large hydrophobic pocket on the core of Nef [10,11]. It is likely that the N-terminal arm makes other functionally important interactions with the core region of the protein. In order to investigate the interactions of the N-terminal arm with the structural core of Nef we made a series of truncation and point mutants in the N-terminal arm and evaluated their structural energetics using high sensitivity differential scanning calorimetry (DSC).

2. Experimental procedures

2.1. Sample preparation

Nef from the BH10 strain of HIV-1 (residues 1–206) was expressed in *Escherichia coli* using the pET11a expression system from Novagen. The original expression vector was provided by Paul Wingfield with alanine substitutions at residues C55 and C206. Residue 55 was changed back to the naturally occurring cysteine using the Quickchange system (Stratatgene). The last residue of the protein, 206, was left as alanine to avoid aggregation via disulfide bonds. *E. coli* cultures containing the expression vector were grown to an optical density (OD) of 0.6 to 0.8 as measured at 600 nm, and protein expression was induced with IPTG for 6 h. Cells were harvested by centrifugation and lysed by sonication in 100 mM Tris pH 7.4 with 4 mM DTT, 1 mM EDTA and 4 M urea. Cell lysate was treated with PEI to precipitate contaminating DNA and clarified by centrifugation. Clarified lysate was diluted with 50 mM Tris pH 7.4 with 2 mM DTT and 2 M urea and applied to a Q sepharose column (GE Healthcare). Protein was eluted by a salt gradient from 0 to 500 mM NaCl. Fractions containing Nef were identified by Coomassie stained SDS-PAGE and diluted with 50 mM Tris pH 8.0 with 2 mM DTT and 2 M urea. The fractions were then applied to a Source15Q column (GE Healthcare), and protein was eluted by a salt gradient from 0 to 500 mM NaCl. Resulting fractions were evaluated by Coomassie stained SDS-PAGE, and fractions containing Nef were pooled, and the buffer was exchanged to 10 mM HEPES pH 7.2 with 150 mM NaCl to refold the protein. The protein was further purified with a Superdex 75 column (GE Healthcare). The protein was eluted in 10 mM HEPES pH 7.2 with 150 mM NaCl. Nef protein was determined to be pure based on analysis by Coomassie stained SDS-PAGE.

2.2. Differential scanning calorimetry

The heat capacity function of the different Nef constructs was measured as a function of temperature with a high precision differential scanning microcalorimeter VP-DSC (Microcal Inc., Northampton, MA). Protein samples and reference solutions were properly degassed and carefully loaded into the cells to avoid bubble formation. Exhaustive cleaning of the cells was undertaken before each experiment. Thermal denaturation scans were performed with freshly prepared Nef solutions dialyzed into 10 mM Mops pH 8.0 with 1 mM EDTA with a protein concentration of 0.5 mg/ml. Reversibility for a single cycle was at least 80%. Data were analyzed by software developed in this laboratory.

2.3. Proteolytic cleavage of Nef

Proteolytic cleavage of Nef by HIV protease occurs at the site located between residues 60 and 61. Purified Nef was incubated overnight with HIV protease in 10 mM Mops pH 6.5 with 1 mM DTT. The N-terminus of Nef was removed using a Q sepharose column. The C-terminal part of Nef binds to the column and can be eluted with salt, while the N-terminal part does not bind the column. The cleavage site was verified by N-terminal sequencing of the protein.

2.4. Generation of Nef mutants

The expression vector for Δ40 Nef (residues 40 to 206) was provided by Paul Wingfield. All other point mutants and truncations were generated using the Quickchange system from Stratagene. All mutants were made from the C55, A206C construct described above. Expression and purification of mutant proteins were accomplished using the same protocol as described above. A summary of the Nef constructs is shown

in Table 2. Truncation mutants are named for the first residue present in the construct excluding methionine.

3. Results

3.1. Full length and HIV-1 protease-cleaved Nef

The temperature dependence of the excess heat capacity function of full length Nef (FL-Nef) is shown in Fig. 2. The thermal denaturation of FL-Nef is centered at 53.6 °C and characterized by an enthalpy change (ΔH) of 112 kcal/mol and a heat capacity change (ΔC_p) of 1.4 kcal/K mol. The transition is 89% reversible as indicated by repeated scans of the same sample (the situation is similar for all the constructs used in these studies). As shown in the figure, the transition is accounted well by the two-state mechanism, as also indicated by a van't Hoff to calorimetric enthalpy ratio ($\Delta H_{vH}/\Delta H$) of 1.1. At 25 °C the structural stability of FL-Nef is characterized by a Gibbs energy (ΔG) of 8.0 kcal/mol. All thermodynamic parameters are summarized in Table 1.

Nef contains a naturally occurring HIV-1 protease cleavage site that removes the majority of the N-terminal arm. N-terminal sequencing of the protease cleaved Nef (61-Nef) indicates a single cleavage site between residues A60 and Q61. The heat capacity function of 61-Nef is shown in Fig. 3A. The transition also obeys the two-state mechanism but the denaturation temperature is shifted downwards by 9° to 44.8 °C. The enthalpy change of 61-Nef is 70 kcal/mol with a ΔC_p of 1.0 kcal/K mol (summarized in Table 1). Preliminary results were presented in Ref. [14]. It is obvious that the N-terminal arm (residues 1–60) contributes significantly to the structural stability of Nef and that this arm cannot be considered as a non-interacting tail hanging lose from the core structure. In fact, it not only contributes to the stability of the core but provides additional structure as demonstrated by the measured enthalpy changes. The difference of 42 kcal/mol for a temperature decrease of 9 °C is much larger than the one expected from the ΔC_p of FL-Nef. If the only effect of the removal of the N-terminus were a destabilization of the same structure, a ΔH of

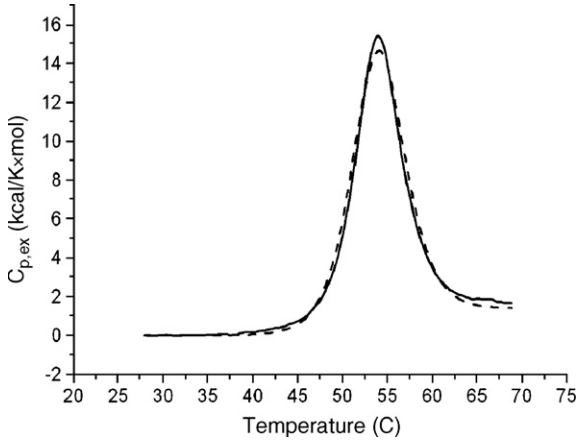

Fig. 2. The excess heat capacity function of FL-Nef. The experimental data is shown in solid black, and the fit to a two-state transition is shown as a dotted line.

Table 1
Thermodynamic values of Nef truncations obtained from DSC

Nef construct	T_m (°C)	ΔH (kcal/mol)	ΔC_p (kcal/K mol)	$\Delta G_{25\ °C}$ (kcal/mol)	$\Delta\Delta G_{25\ °C}$ (kcal/mol)
FL-Nef	53.6	112	1.4	8.0	NA
61-Nef	44.8	70	1.0	3.7	−4.3
40-Nef	49.6	98	1.0	6.4	−1.6
45-Nef	49.7	97	0.92	6.5	−1.5
49-Nef	49.9	93	1.0	6.2	−1.8

96 kcal/mol would have been expected. The reduction in stability of 61-Nef compared to FL-Nef is also apparent in a reduced Gibbs energy of stabilization as shown in Fig. 3B. At 25 °C the ΔG of 61-Nef is 3.7 kcal/mol compared to 8.0 kcal/mol for FL-Nef. These results indicate that the N-terminus of Nef interacts strongly with the core and as a result, the full length protein defines a single cooperative entity involving the core as well as the N-terminus. An important question that arises from these experiments relates to the number and identity of the amino acids responsible for this interaction since some of the

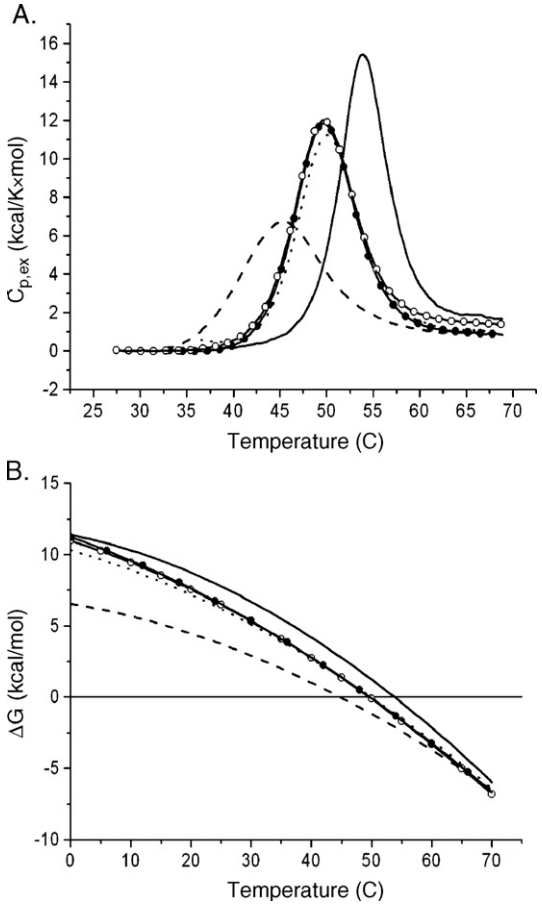

Fig. 3. (Panel A) Comparison of the excess heat capacity function for the truncation mutants of Nef. FL-Nef is shown in a solid black line while 61-Nef is a dashed line, 40-Nef is marked with open circles, 45-Nef is marked with closed circles and 49-Nef is a dotted line. (Panel B) Comparison of the ΔG versus temperature for the truncated forms of Nef. FL-Nef is shown in black while 61-Nef is dashed line, 40-Nef is marked with open circles, 45-Nef is marked with closed circles and 49-Nef is a dotted line.

Table 2
Summary of Nef constructs

Nef construct	Residues	Mutation
FL-Nef	1–206	–
61-Nef	61–206	–
40-Nef	1, 40–206	–
45-Nef	1, 45–206	–
49-Nef	1, 49–206	–
W57A	1–206	W57A
L458A	1–206	L58A
A56D	1–206	A56D
C55A	1–206	C55A
W57A/L58A	1–206	W57A/L58A
C55A/W57A	1–206	C55A/W57A

residues in the N-terminal arm appear rather flexible in NMR experiments [10,11].

3.2. Sequential truncations of the N-terminal arm of Nef

The regions in the N-terminal arm that are important for its interaction with the core region were identified by measuring the structural stability and energetics of several sequential truncations (Table 2). The excess heat capacity function for the Nef truncation beginning with residue 40 (40-Nef) is shown with open circles in Fig. 3A. 40-Nef also undergoes two state thermal unfolding centered at 49.6 °C with a ΔH of 98 kcal/mol and a ΔC_p of 1.0 kcal/K mol. These values are intermediate between those obtained for FL-Nef and 61-Nef. At 25 °C the Gibbs energy of 40-Nef is 1.6 kcal/mol lower than that of FL-Nef (Table 1, Fig. 3B). The change in ΔG resulting from the truncation of residues 2–40 indicates that the interactions between the far N-terminus and the core of the protein contribute 1.6 kcal/mol, while the region between residues 41 and 60 contribute close to 2.7 kcal/mol to the Gibbs energy of stabilization.

Comparison of 40-Nef with additional truncations at residues 45 and 49, shown in Fig. 3A–B, reveal no significant difference in stability suggesting that residues 40–49 contribute little to the FL-Nef structure. A comparison of the $\Delta\Delta G$ for all the truncation mutants is shown in Fig. 4. The figure clearly indicates that the most important interactions are concentrated between residues 1–40 and residues 50–61.

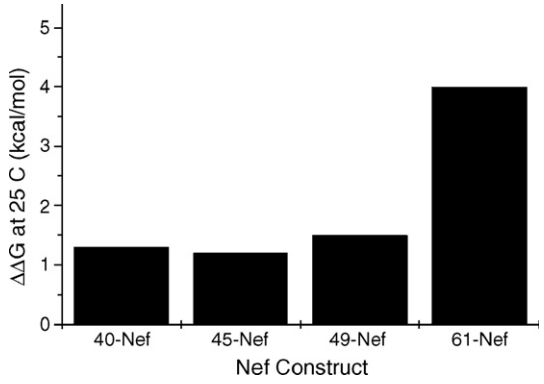

Fig. 4. Comparison of the changes in ΔG at 25 °C for different truncations of Nef. The bar graph shows the $\Delta\Delta G$ values in kcal/mol relative to full length Nef.

3.3. Effects of point mutations on the stability of Nef

Since the region between residues 50 and 61 appears to be important in contributing to the stability of Nef, point mutations were made in this region in order to evaluate the contribution of specific residues. The point mutations are listed in Table 2. All of them are Ala mutations except for the naturally occurring Ala 56 which was mutated to Asp. Fig. 5A shows the excess heat capacity function for C55A, A56D, W57A, and L58A. The unfolding transition of all four mutants also obeys the two-state mechanism. The thermodynamic parameters are summarized in Table 3. It is evident that the mutants A56D, W57A and L58A show no significant shift in T_m with respect to wild-type Nef, suggesting that these residues do not provide a major contribution to the N-terminus/core interaction within the transition region. On the contrary, the mutant C55A shows a decrease in T_m of almost 4°, suggesting a strong contribution of this residue.

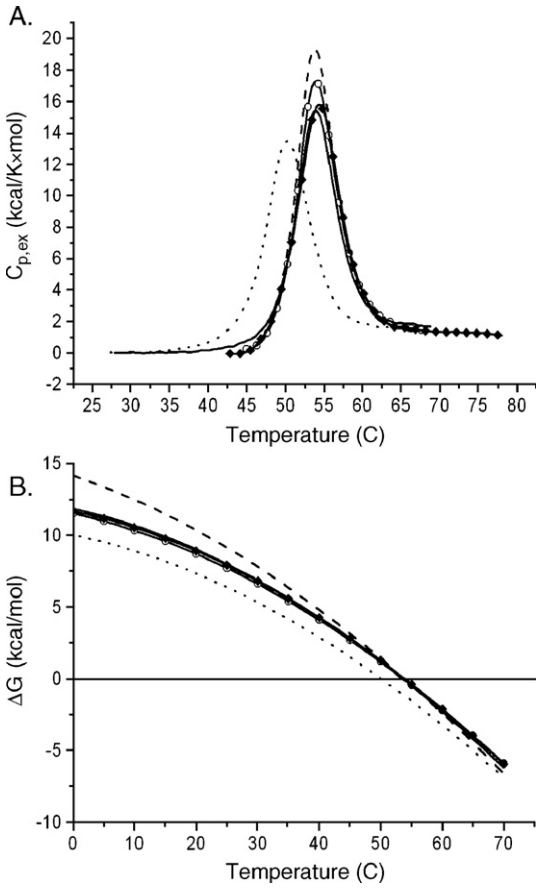

Fig. 5. (Panel A) Comparison of the excess heat capacity curves for the point mutations of Nef. FL-Nef is shown in black while W57A is shown as a dashed line, L58A is marked with open circles, A56D is shown with diamonds and C55A is shown as a dotted line. (Panel B) Comparison of the ΔG versus temperature for the point mutants of Nef. FL-Nef is shown in black while W57A is shown as a dashed line, L58A is marked with open circles, A56D is shown with diamonds and C55A is shown as a dotted line.

Table 3
Thermodynamic values of Nef point mutations obtained from DSC

Nef construct	T_m (°C)	ΔH (kcal/mol)	ΔC_p (kcal/K mol)	$\Delta G_{25\ °C}$ (kcal/mol)	$\Delta\Delta G_{25\ °C}$ (kcal/mol)
FL-Nef	53.6±0.2	112±4	1.4±0.1	8.0±0.3	NA
C55A	50.1±0.1	99±2	1.3±0.1	6.3±0.2	−1.7
A56D	54.1±0.01	110±3	1.4±0.1	8.0±0.4	0
W57A	53.8±0.01	123±2	1.3±0.2	8.9±0.4	0.9
L58A	53.6±0.3	107±8	1.3±0.2	7.7±0.8	−0.3
W57A/L58A	53.8±0.02	116±3	1.3±0.03	8.5±0.4	0.5
C55A/W57A	50.3±0.09	109±5	1.3±0.05	7.2±0.5	−0.8

A closer inspection of the thermodynamic data in Table 3 reveals that the mutant W57A exhibits slightly larger denaturation enthalpy despite showing the same denaturation temperature as FL-Nef. In fact, when the Gibbs energy is calculated (Fig. 5B) the mutant W57A shows an increased stability at 25 °C by approximately 1 kcal/mol. The A56D and L58A mutants show no change from FL-Nef. The C55A mutant, on the other hand, shows a decreased ΔG at 25 °C (−1.7 kcal/mol) similar to the decrease in stability seen upon truncation of the first 39 residues of Nef (Tables 2 and 3).

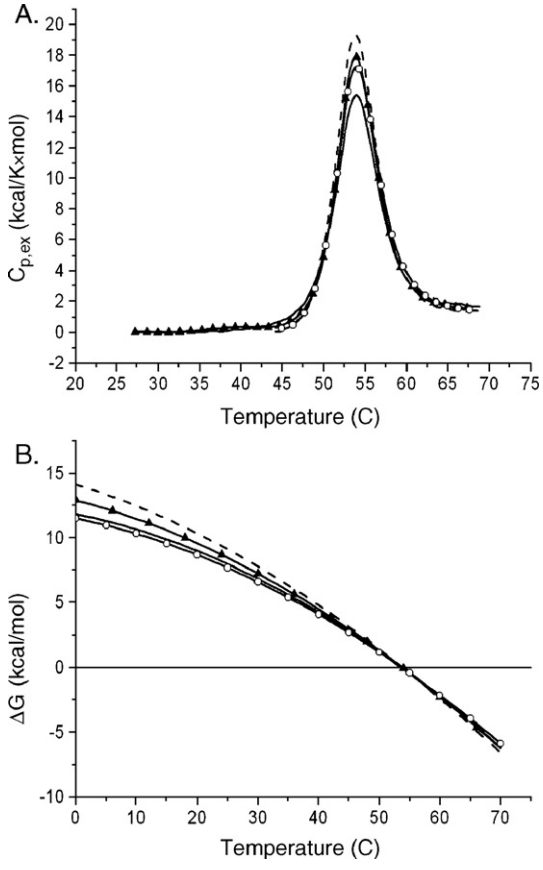

Fig. 6. (Panel A) The excess heat capacity function of W57A/L58A compared to FL-Nef, W57A and L58A. The double mutant is marked with triangles, and FL-Nef is in black. The single mutants are shown as a dashed line (W57A) and marked with open circles (L58A). (Panel B) Comparison of ΔG versus temperature for W57A/L58A. W57A/L58A is marked with triangles, and FL-Nef is in black. The single mutants are shown as a dashed line (W57A) and marked with open circles (L58A).

3.4. The effect of double mutants on the stability of Nef

The double mutant W57A/L58A has been shown to prevent down-regulation of the CD4 receptor in vivo [20]. The effect of these two mutations on the structural stability of Nef is shown in Fig. 6A. The double mutant undergoes a two-state unfolding transition centered at 53.8 °C with a calorimetric enthalpy of 116 kcal/mol and a heat capacity change of 1.3 kcal/K mol. While the T_m is similar to the one observed for FL-Nef, the denaturation enthalpy is 4 kcal/mol larger. Individually, W57A induces an enthalpy increase of 11 kcal/mol while L58A induces a decrease of 5 kcal/mol. It seems that the enthalpic effects of these mutations are largely additive.

Since the alanine substitution for C55 was the only mutation in this region that reduced the stability of Nef, the effect of mutating both C55 and W57 was also studied (Fig. 7A). The C55A/W57A undergoes a two-state unfolding transition centered at 50.3 °C with a calorimetric enthalpy of 109 kcal/mol and a heat capacity change of 1.3 kcal/K mol. The denaturation temperature of the double mutant is similar to that of the C55A single mutant which is about 3.5 °C lower than FL-Nef (Table 3). However, the increased in ΔH observed for the W57A single mutant is also observed in the double mutant. The

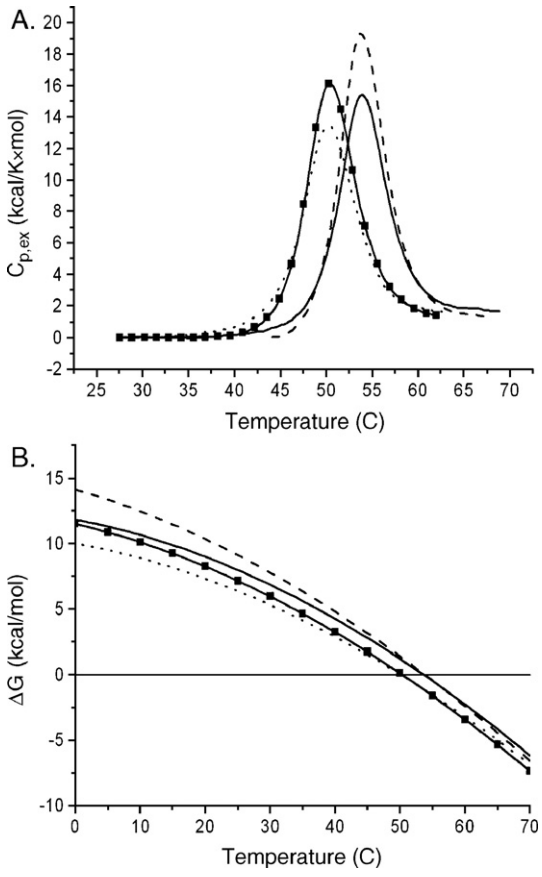

Fig. 7. (Panel A) The excess heat capacity function of C55A/W57A compared to FL-Nef, C55A, and W57A. The double mutant is marked with closed squares, and FL-Nef is in black. The single mutants are shown as a dashed line (W57A) and a dotted line (C55A).

net result is a mutually compensating set of mutations that result in no significant stability change at 25 °C.

4. Discussion

The calorimetric results presented here demonstrate the presence of strong interactions between the N-terminal arm and the structural core of Nef. Analysis of the thermodynamic parameters for the sequential truncations in the N-terminal arm reveals the presence of strong interactions of the protein core with the far N-terminus of Nef (residues 1–40) and with residues nearer in sequence to the polyproline helix (residues 49 to 60). Based on the NMR structure of Nef, it is not surprising that the region between residues 49 and 60 will have a significant influence on the stability of the protein. According to the NMR data, the N-terminal arm appears to be highly flexible with the exception of a region centered around W57 [11]. The thermodynamic effects reported here reflect overall energetic contributions triggered by the different mutations or truncations; as such they cannot be necessarily attributed to the interactions of specific amino acids since long range cooperative effects involving other residues may be present.

The interactions between the far N-terminus (residues 1–40) are not present in any of the available structures since truncated forms of the protein were used for structure determination in all cases [9–12]. The observed changes in ΔG from the truncation of residues 2–40 indicate that the interactions between the far N-terminus and the core of the protein contribute 1.6 kcal/mol, while the region between residues 41 and 60 contribute close to 2.7 kcal/mol to the Gibbs energy of stabilization. Both sets of interactions are significant and suggest that the entire N-terminal arm establishes a strong interaction with the protein core. The fact that the interaction energy is not evenly spread over the entire arm allows for regions of flexibility.

The NMR structure of Nef shows that W57 and L58 are buried in a large hydrophobic pocket on the surface of the protein [10,11]. Mutation of W57 to the small hydrophobic residue Ala results in no change in denaturation temperature but a significant increase in the enthalpy change. It appears that a predominantly hydrophobic interaction is replaced by a polar one, perhaps due to the elimination of steric constraints that originate from the larger size of the indole group in the Trp side chain. At the thermodynamic level, the net effect is a clear case of enthalpy/entropy compensation that results in no change in denaturation temperature. However, due to the different temperature dependencies, the higher enthalpy change at T_m results in a higher structural stability at lower temperatures. A higher structural stability at physiological temperatures implies a higher energy penalty for any Nef interaction that requires separation of the N-terminal arm from the core. Consistent with these results, in vivo data for W57A and L58A show a disruption of the down-regulation of CD4 [19,20]. Even though C55 does not participate in any disulfide bridge, it appears to be a major contributor to the N-terminal arm interaction with the core, judging by the major decrease in stability observed for the C55A mutant.

Acknowledgements

This work was supported by grants from the National Science Foundation MCB0131241 and the National Institutes of Health GM 57144 and GM56550.

References

[1] H.W. Kestler III, D.J. Ringler, K. Mori, D.L. Panicali, P.K. Sehgal, M.D. Daniel, R.C. Desrosiers, Importance of the Nef gene for maintenance of high virus loads and for development of AIDS, Cell 65 (1991) 651–662.
[2] F. Kirchhoff, T.C. Greenough, D.B. Brettler, J.L. Sullivan, R.C. Desrosiers, Brief report—absence of intact Nef sequences in a long-term survivor with nonprogressive HIV-1 infection, New Engl. J. Med. 332 (1995) 228–232.
[3] Z. Hanna, D.G. Kay, N. Rebai, A. Guimond, S. Jothy, P. Jolicoeur, Nef harbors a major determinant of pathogenicity for an AIDS-like disease induced by HIV-1 in transgenic mice, Cell 95 (1998) 163–175.
[4] X. Liu, J.A. Schrager, G.D. Lange, J.W. Marsh, HIV Nef-mediated cellular phenotypes are differentially expressed as a function of intracellular Nef concentrations, J. Biol. Chem. 276 (2001) 32763–32770.
[5] J.W. Marsh, The numerous effector functions of Nef, Arch. Biochem. Biophys. 365 (1999) 192–198.
[6] M.Y. Chowers, C.A. Spina, T.J. Kwoh, N.J. Fitch, D.D. Richman, J.C. Guatelli, Optimal infectivity in vitro of human immunodeficiency virus type 1 requires an intact Nef gene, J. Virol. 68 (1994) 2906–2914.
[7] S.D. Briggs, B. Scholtz, J.M. Jacque, S. Swingler, M. Stevenson, T.E. Smithgall, HIV-1 Nef promotes survival of myeloid cells by a Stat3-dependent pathway, J. Biol. Chem. 276 (2001) 25605–25611.
[8] Z. Hanna, E. Priceputu, D.G. Kay, J. Poudrier, P. Chrobak, P. Jolicoeur, In vivo mutational analysis of the N-terminal region of HIV-1 Nef reveals critical motifs for the development of an AIDS-like disease in CD4C/HIV transgenic mice, Virology 327 (2004) 273–286.
[9] S. Arold, P. Franken, M.P. Strub, F. Hoh, S. Benichou, R. Benarous, C. Dumas, The crystal structure of HIV-1 Nef protein bound to the Fyn kinase SH3 domain suggests a role for this complex in altered T cell receptor signaling, Structure 5 (1997) 1361–1372.
[10] S. Grzesiek, A. Bax, G.M. Clore, A.M. Gronenborn, J.S. Hu, J. Kaufman, I. Palmer, S.J. Stahl, P.T. Wingfield, The solution structure of HIV-1 Nef reveals an unexpected fold and permits delineation of the binding surface for the SH3 domain of Hck tyrosine protein kinase, Nat. Struct. Biol. 3 (1996) 340–345.
[11] S. Grzesiek, A. Bax, J.S. Hu, J. Kaufman, I. Palmer, S.J. Stahl, N. Tjandra, P.T. Wingfield, Refined solution structure and backbone dynamics of HIV-1 Nef, Protein Sci. 6 (1997) 1248–1263.
[12] C.H. Lee, K. Saksela, U.A. Mirza, B.T. Chait, J. Kuriyan, Crystal structure of the conserved core of HIV-1 Nef complexed with a Src family SH3 domain, Cell 85 (1996) 931–942.
[13] S.T. Arold, A.S. Baur, Dynamic Nef and Nef dynamics: how structure could explain the complex activities of this small HIV protein, Trends Biochem. Sci. 26 (2001) 356–363.
[14] S.A. Leavitt, A. Schon, J.C. Klein, U. Manjappara, I.M. Chaiken, E. Freire, Interactions of HIV-1 proteins gp120 and Nef with cellular partners define a novel allosteric paradigm, Curr. Protein Pept. Sci. 5 (2004) 1–8.
[15] S. Grzesiek, S.J. Stahl, P.T. Wingfield, A. Bax, The CD4 determinant for downregulation by HIV-1 Nef directly binds to Nef. Mapping of the Nef binding surface by NMR, Biochemistry 35 (1996) 10256–10261.
[16] S. Salghetti, R. Mariani, J. Skowronski, Human-immunodeficiency-virus type-1 Nef and P56(Lck) protein–tyrosine kinase interact with a common element in Cd4 cytoplasmic tail, Proc. Natl. Acad. Sci. U. S. A. 92 (1995) 349–353.
[17] S.R. Das, S. Jameel, Biology of the HIV Nef protein, Indian J. Med. Res. 121 (2005) 315–332.
[18] J. Lama, The physiological relevance of CD4 receptor down-modulation during HIV infection, Curr. HIV Res. 1 (2003) 167–184.

[19] R. Mariani, F. Kirchhoff, T.C. Greenough, J.L. Sullivan, R.C. Desrosiers, J. Skowronski, High frequency of defective Nef alleles in a long-term survivor with nonprogressive human immunodeficiency virus type 1 infection, J. Virol. 70 (1996) 7752–7764.
[20] C.A. Stoddart, R. Geleziunas, S. Ferrell, V. Linquist-Stepps, M.E. Moreno, C. Bare, W.D. Xu, W. Yonemoto, P.A. Bresnahan, J.M. McCune, W.C. Greene, Human immunodeficiency virus type 1 Nef-mediated down-regulation of CD4 correlates with Nef enhancement of viral pathogenesis, J. Virol. 77 (2003) 2124–2133.
[21] S. Arold, R. O'Brien, P. Franken, M.P. Strub, F. Hoh, C. Dumas, J.E. Ladbury, RT loop flexibility enhances the specificity of Src family SH3 domains for HIV-1 Nef, Biochemistry 37 (1998) 14683–14691.